Received: 18 November 2022 | Revised: 17 January 2023 | Accepted: 27 January 2023

DOI: 10.1002/ar.25176

SPECIAL ISSUE ARTICLE

The Anatomical Record WILEY

Hair, there and everywhere: A comparison of bat wing sensory hair distribution

Andrea D. Rummel[1,2] | **Melissa M. Sierra**[1] | **Brooke L. Quinn**[1] | **Sharon M. Swartz**[1,3]

[1]Department of Ecology, Evolution, and Organismal Biology, Brown University, Providence, Rhode Island, USA

[2]Department of Ecology and Evolutionary Biology, Princeton University, Princeton, New Jersey, USA

[3]School of Engineering, Brown University, Providence, Rhode Island, USA

Correspondence
Andrea D. Rummel, Department of Ecology and Evolutionary Biology, Princeton University, Princeton, NJ 08544, USA.
Email: arummel25@gmail.com

Funding information
Air Force Office of Scientific Research, Grant/Award Number: FA9550-11-C-0028; NDSEGFellowship, Grant/Award Number: 32CFR168a; National Science Foundation, Grant/Award Numbers: CMMI 1426338, IOS 1931135; Brown University Undergraduate Teaching and Research Award; Bushnell Research and Education Fund

Abstract

Bat wing membranes are composed of specialized skin that is covered with small sensory hairs which are likely mechanosensory and have been suggested to help bats sense airflow during flight. These sensory hairs have to date been studied in only a few of the more than 1,400 bat species around the world. Little is known about the diversity of the sensory hair network across the bat phylogeny. In this study, we use high-resolution photomicrographs of preserved bat wings from 17 species in 12 families to characterize the distribution of sensory hairs along the wing and among species. We identify general patterns of sensory hair distribution across species, including the apparent relationships of sensory hairs to intramembranous wing muscles, the network of connective tissues in the wing membrane, and the bones of the forelimb. We also describe distinctive clustering of these sensory structures in some species. We also quantified sensory hair density in several regions of interest in the propatagium, plagiopatagium, and dactylopagatia, finding that sensory hair density was higher proximally than distally. This examination of the anatomical organization of the sensory hair network in a comparative context provides a framework for existing research on sensory hair function and highlights avenues for further research.

KEYWORDS

bat, flight, sensorimotor integration, sparse sensing, wing membrane

1 | INTRODUCTION

Bats are agile and highly maneuverable fliers. They navigate complex aerial environments using modified forelimbs as wings. Specialized skin that stretches between the bones of the arm, forearm, hand, and hindlimb comprises the aerodynamic surface of the wing and is flexible in multiple ways. This wing membrane is covered with small hairs that receive sensory innervation, that likely serve a mechanosensory function, and that have been proposed to sense airflow during flight (Sterbing-D'Angelo & Moss, 2014). The anatomical organization of wing sensory structures suggests that information from aerodynamically significant regions of the wing may be involved in the neural control of the motor system in insects and birds (Altshuler et al., 2015; Dickinson et al., 1997; Jones, 2011). The hair-dome complexes consist of fine hairs (~5–25 μm in diameter) which extend from epidermally embedded mechanosensory Merkel

Andrea D. Rummel and Melissa M. Sierra contributed equally to this study.

cells (Crowley & Hall, 1994; Marshall et al., 2015; Sterbing & Moss, 2018). Merkel cells are particularly sensitive to pressure, enable interpretation of shapes and textures, and are known to respond to the expansion of neighboring cells, as might be induced by stretching the skin (Owens & Lumpkin, 2014). In bats, hair length increases with body size and varies with wing region, increasing distally and toward the trailing edge. Removal of the small (<1 mm length) wing hairs resulted in increased flight speed and wider turns compared to the control condition in flight experiments with the species *Carollia perspicillata* and *Eptesicus fuscus*, suggesting that the hairs play a role in maneuvering (Sterbing & Moss, 2018; Sterbing-D'Angelo et al., 2011, 2017). To date, research concerning bat wing sensory hairs has focused on species commonly studied in laboratory environments (Sterbing-D'Angelo et al., 2011, 2016, 2017; Sterbing-D'Angelo & Moss, 2014; Zook, 2005), leaving much of the diversity of bats unexplored.

Descriptors of the wings such as aspect ratio or wing loading have often been used to estimate maneuverability, but provide limited information about flight performance capabilities for animals with numerous wing joints and sophisticated motor control. The distribution of sensors over the wings has the potential to convey additional pertinent information about the sensory pathways that provide data to the central nervous system that may then influence muscle activation patterns to fine-tune a bat's wing shape. For example, camber, controlled at least in part by activity of intramembranous muscles and by handwing joint flexion/extension, varies along the wingspan and over the time course of the wingbeat cycle (Cheney et al., 2022; Fan et al., 2022; Stockwell, 2001). Because of this spatial and temporal variation, along with wing membrane skin anisotropy, the information conveyed to the CNS from wing skin sensors may be strongly influenced by the placement of sensory structures. Previous studies provide insight into sensory hair function, and raise many more questions about the function, morphological diversity, distribution, and evolution of these structures. Among the most basic, we ask: how are sensory hairs distributed in the wing, and is sensory hair distribution functionally significant? Is the distribution of sensory hairs in the wing comparable in diverse species? To address these questions, in this study we characterize wing sensory hair distribution in 17 bat species from 12 families, a sample that represents a broad range of habitats and feeding ecologies. We address two main hypotheses: (a) sensory hair density (hairs/cm^2) varies among regions of the wing and (b) sensory hair density varies among species. We describe qualitatively the distribution and patterning of sensory hairs across the wing, and quantify sensory hair density (hair number/surface area) in several specific wing regions of interest (ROIs). This analysis provides a framework for understanding the morphological diversity and functional significance of an important sensory system in bats, the only mammals capable of flapping flight.

2 | METHODS

2.1 | Study sample

We imaged 72 bat specimens from 17 species and 12 families. Sixty-three specimens were loaned from the American Museum of Natural History, and nine were collected by the Swartz Lab from the Lamanai Archeological Preserve in Orange Walk, Belize (Belize Forestry Department Scientific Research and Collecting Permits CD/60/3/15 (14) and WL/2/1/17(16), Table S1). We selected one or more species within each family represented in the sample for in-depth study based on specimen quality and availability, as well as body size appropriate for the size constraints of the microscopy method. All specimens had been previously formalin-fixed and stored in ethanol. Each species' dietary preferences were obtained by literature review (Figure 1 and Table S2).

2.2 | Imaging

To lay each wing as flat as possible for imaging, we fully extended the right or left wing, ventral surface up, and

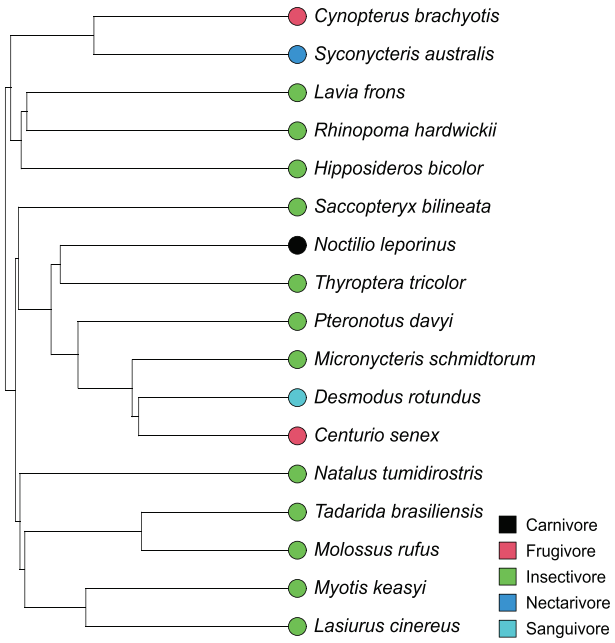

FIGURE 1 Phylogenetic relationships of all species used in this study, and their predominant diet category.

gently pinned it along the wing bones to a soft and nearly transparent gelatin base, taking care to avoid or minimize damage to the wing membrane. If necessary, the wing was dissected from the body of the specimen to ensure it lay flat against the gelatin. We viewed and captured images from these extended-wing specimens with a Nikon SMZ800 dissecting scope outfitted with a Nikon DXM1200C digital camera. We illuminated specimens with a 400–460 nm wavelength lamp, and a filter mount attached to the microscope eliminated light wavelengths above 500 nm. Elastin and collagen autofluoresce in the near ultraviolet and into the visible range (Bachmann et al., 2006; Monici, 2005). Thus, structures composed of these proteins appeared bright green against a dark background. Each wing was photographed with an approximately 10 by 8 mm linear scale within the field of view. We collected multiple overlapping digital photomicrographs of each specimen and then stitched them in Adobe Photoshop to create a photo composite of the whole wing. We analyzed the composites in ImageJ (see Appendix S1 for photo composites of each study species).

2.3 | Sensory hair analysis and quantification

We identified patterns in sensory hair arrangement and density variation within and among species by focusing on apparent associations of the sensory hairs with other wing structures, such as intramembranous muscles in the plagiopatagium (Figure 2), elastin bundles, and the wing skeleton, especially the bones of the handwing. We identified relevant qualitative descriptive categories, for example, "clustering," "morphology association," and "density," and sorted both species and wing regions accordingly. In addition to this descriptive survey, we counted sensory hairs using ImageJ. We sampled ROIs in each membrane region along the wing's proximodistal axis, from the proximal plagiopatagium and propatagium to the dactylopatagium medius (Figure 3). The hairs were associated with dome-like receptors in the wing membrane (Crowley & Hall, 1994; Sterbing-D'Angelo et al., 2016). The domes, which also fluoresce, were more clearly distinguishable for the purpose of counting than the finer hairs, and we assumed that the presence of a dome indicated at least one associated sensory hair, although individual domes can be associated with multiple hairs. We identified hairs or the domes associated with them by their contrast with the background skin, marked each with the point tool and counted the marked points in each sample area.

Most ROIs were circular samples of the wing membrane scaled to forearm length; the diameter of each ROI was set to a quarter of the distance from the tip of the olecranon process (proximal forearm) to the proximal end of metacarpal III (distal wrist) (Figure 3). We established one cranially and one caudally located ROI in each of the following wing membrane regions: proximal plagiopatagium, distal plagiopatagium, dactylopatagium major, and dactylopatagium medius (Figure 3). The ROIs were selected to give good coverage of the full wing surface, and to provide additional focus on wing regions hypothesized to play a particularly large role in sensing airflow or wing strain. We counted all hairs in the propatagium because its area is relatively small and it is likely to play a key role in flight dynamics. Presence, absence, and density of hairs within an ROI were indicative of the distribution of hairs within a wing region overall, however, these measurements do not represent a comprehensive assessment of sensory hair distribution across the entirety of the wing region. For example, hairs may be

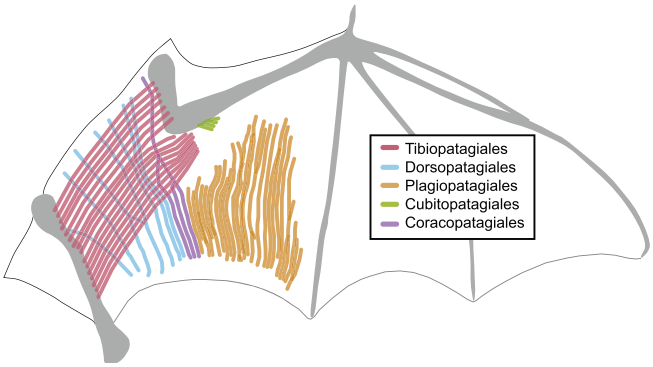

FIGURE 2 The locations of the intramembranous muscles in the bat wing. *Source*: Modified from Cheney et al. (2017).

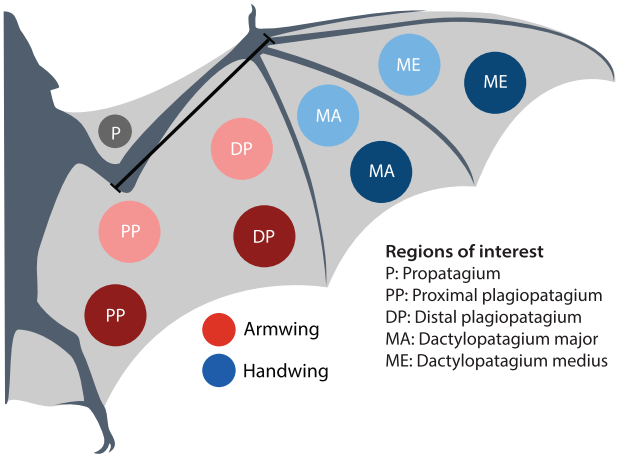

FIGURE 3 Labeled regions of interest (ROIs). Cranial and caudal wing regions are shown in lighter and darker colors, respectively. Armwing and handwing regions are shown in red and blue. The distance used to calculate the area of the regions of interest is indicated by the black line along the forearm.

TABLE 1 Mean number of sensory hairs per cm^2 measured in each region of interest for each species.

Species	Cranial Prox. Plagio.	Caudal Prox. Plagio.	Propatagium	Cranial Dist. Plagio.	Caudal Dist. Plagio.	Caudal Dactylo. Major	Cranial Dactylo. Major	Caudal Dactylo. Medius	Cranial Dactylo. Medius	Prox. Mean	Dist. Mean	Cranial mean	Caudal mean
Centurio senex	327.33	168.96	376.89	370.51	266.70	652.48	554.78	79.11	2.72	283.38	322.27	287.89	317.76
Cynopterus brachyotis	117.84	159.43	168.22	116.74	42.38	34.71	36.36	50.87	28.80	109.10	37.69	56.34	90.44
Desmodus rotundus	241.76	199.99	326.86	85.16	59.77	8.78	20.28	15.82	21.52	146.67	16.60	85.83	77.43
Hipposideros bicolor	94.68	135.45	172.77	128.10	84.04	124.37	111.96	136.13	134.70	110.57	126.79	106.35	131.01
Lasiurus cinereus	191.73	184.33	274.48	58.61	137.21	51.79	58.01	48.06	64.22	142.97	55.52	112.79	85.70
Lavia frons	81.58	15.44	94.92	11.63	33.66	26.63	49.76	19.69	23.93	35.58	30.00	47.23	18.35
Micronycteris schmidtorum	149.44	193.28	396.53	248.05	270.82	167.41	186.39	177.84	165.87	215.40	174.38	193.13	196.65
Molossus rufus	1,182.83	3,079.22	1,067.37	812.40	1,272.40	563.88	745.88	115.82	279.69	1,586.71	426.32	870.20	1,142.83
Myotis keaysi	162.89	189.09	174.56	114.69	96.40	102.92	112.18	173.00	82.67	140.77	117.69	113.54	144.92
Natalus tumidirostris	70.68	130.72	164.22	167.35	80.86	136.86	96.36	170.63	108.65	112.40	128.13	89.14	151.39
Noctilio leporinus	38.78	24.81	128.44	48.56	72.48	31.14	33.62	19.56	29.71	46.16	28.51	43.65	31.02
Pteronotus davyi	136.01	165.23	195.22	115.43	101.80	111.73	99.05	172.89	92.82	129.62	119.12	107.42	141.32
Rhinopoma hardwickii	338.63	336.70	259.48	348.39	201.65	344.30	246.74	382.86	162.49	306.34	284.10	237.38	353.06
Saccopteryx bilineata	243.53	179.35	461.13	99.69	140.51	111.69	97.16	25.92	69.76	165.77	76.13	137.74	104.16
Syconycteris australis	65.03	95.16	81.36	27.56	26.03	11.21	31.37	6.60	18.54	53.44	16.93	35.24	35.13
Tadarida brasiliensis	1,179.79	822.20	759.08	759.15	1,082.63	242.72	430.64	110.38	226.29	960.94	252.51	729.84	483.61
Thyroptera tricolor	143.68	144.30	133.12	123.34	50.21	110.30	28.05	128.67	32.71	115.39	74.93	63.67	126.65

completely absent within an ROI but present elsewhere in the region it samples. Although the uropatagium is likely important in flight and prey capture, the quality of the tail membranes and ease of imaging varied greatly among specimens so we could not reliably describe or quantify sensory hairs in this wing region. To allow comparisons among bats of greatly varying size, we report areal densities as hair count per cm^2.

2.4 | Statistical analysis

We analyzed sensory hair data in R (R Core Team, 2021). Samples came from 17 species from 12 families, so we tested for phylogenetic signal in our data using the phylosig function in the phytools package (Revell, 2012), using a pruned tree from the time-calibrated phylogeny constructed by Shi and Rabosky (2015) (Figure 1). *Lavia frons* was not included in this published phylogeny, so we assigned it to the phylogenetic position of a closely related species also within the family Megadermatidae that was included in the phylogeny, *Megaderma spasma*.

We evaluated the relationship between wing region, species, and density with a non-phylogenetic linear regression. Because we found significant phylogenetic signal and a significant species effect, we then examined variation among wing regions while accounting for phylogeny. To compare hair density between regions, we performed pairwise comparisons for all regions using phylogenetic *t*-tests and the Bonferroni correction for multiple comparisons. We also evaluated overall differences in proximal and distal densities and cranial and caudal densities by grouping ROIs to explore general trends in sensory hair density in the wing. To compare proximal versus distal, we took the mean values for all ROIs in the plagiopatagium and the handwing, respectively (excluding the propatagium) and to compare cranial versus caudal, we took the mean values of all the cranial (excluding the propatagium) and caudal ROIs (Figure 3 and Table 1). We then performed non-phylogenetic and phylogenetic *t*-tests (Revell, 2012). Because the molossids were outliers, responsible for much of the total sample variance, we repeated the phylogenetic analysis described above after removing *Tadarida brasiliensis* and *Molossus rufus* from the sample; this did not change the results, so we present only results with all species included here.

We used a phylogenetic generalized least squares (PGLS) regression (using the pgls function in the package caper, Orme et al., 2018) to assess significant relationships between hair density and ecological categories. PGLS allows for only one data point per species, so we used phylogenetic principal component analysis (phyl. pca) to reduce the nine wing region variables into one summary variable (phytools package, Revell, 2012). PC1 explained 70% of total variance, so we used PC1 as the response variable in phylogenetic regressions with feeding guild and prey mobility as predictor variables.

3 | RESULTS

3.1 | Density

The arrangement, distribution, and areal density of sensory hairs on the ventral surface of bat wings varied substantially across species. Generally, patterns of sensory hair distribution were similar among individuals within a species (see Appendix S1 for images of multiple *Lasiurus cinereus* and *Centurio senex* specimens). Overall, the density of hairs was higher proximally and decreased distally along the wing. Qualitatively, we observed the highest density in the plagiopatagium. In some species, there was an increase in the density of domes and concentration of elastin fibers along the trailing edge, often accompanied by a decrease in the size of the domes (e.g., *Thyroptera tricolor*, Figure 4). In other cases, as in *Pteronotus davyi* and *Saccopteryx bilineata*, dome density was lower near the trailing edge.

In our non-phylogenetic analysis, wing region, species, and their interaction were significant predictors of sensory hair density (linear regression, $F_{152,491} = 10.74$, $R^2 = 0.70$, $p < .001$). The means of pooled proximal and distal regions (see Section 2) were significantly different, with sensory hair density being higher in the proximal half of the wing (paired *t* test, $p = .009$; mean proximal density = 284 hairs per cm^2, mean distal density = 138 hairs per cm^2); there was no significant difference between the pooled cranial and caudal regions (paired

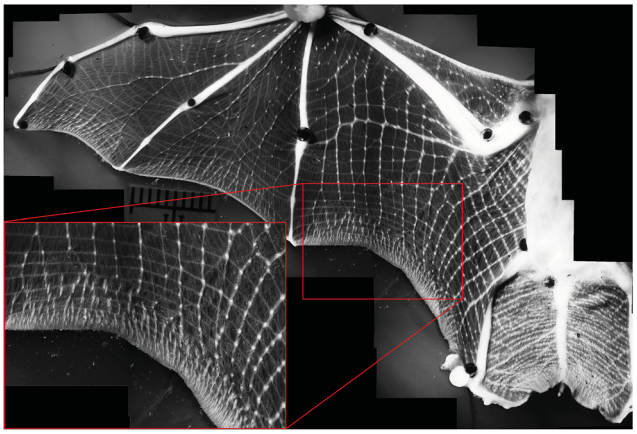

FIGURE 4 The wing of *Thyroptera tricolor* with inset showing high density of sensory hairs along trailing edge.

t test, $p = .67$). When taking phylogenetic relatedness into account, the density of domes was not significantly different between the pooled proximal and distal regions or the pooled cranial and caudal regions. When we evaluated all pairwise comparisons of wing regions within a phylogenetic framework, after Bonferroni correction only the difference in mean density of the propatagium and the cranial dactylopatagium major was significant (phylogenetic *t* test, adjusted $p = .039$), with a higher density in the propatagium. There was no significant relationship between PC1 and feeding guild or prey type (phylogenetic PCA and PGLS).

3.2 | Grouping/clustering

The hairs occur singly, in clusters of a few hairs, or in rosette-like clusters of eight or more hairs (e.g., in the plagiopatagium of molossids, clusters have central domes encircled by additional domes, Figure 5, left inset). Clusters can also be strip-like, comprising many domes and associated hairs in elongated clusters, often oriented craniocaudally (Figure 5, right inset). Clusters were present in a majority of our study species in at least one wing region (excluding *C. senex*, *Cynopterus brachyotis*, *Hipposideros bicolor*, *Lavia frons*, *Micronyceteris schmidtorum*, and *T. tricolor*). Clustering patterns and cluster size often varied across the wing, within even a single specimen (e.g., Figure 5). For example, in the *Noctilio leporinus* propatagium, clusters consist of 3–5 domes, with domes per cluster increasing caudally. In *Natalus tumidorostris* and *Rhinopoma hardwickii*, clusters usually consist of 3 or 4 domes, and in the *Syconycteris australis* propagatium, clusters are tightly grouped and vary in dome density from 3 to 10 domes per cluster. In the proximal plagiopatagium of *Desmodus rotundus*, clusters generally follow muscles with a proximodistal orientation, and remain associated with these muscles as they take on a more craniocaudal orientation near the elbow. By contrast, clusters in *T. brasiliensis* are spread out with no apparent connection to either collagen-elastin bundles or any muscles.

Several species (*L. cinereus*, *M. rufus*, and *T. brasiliensis*) exhibited high densities of domes arranged in strips. In all three species, strips of domes were present in all wing regions studied. The strips run craniocaudally (chordwise) and are often, but not uniformly, near other anatomically significant structures, including intramembranous wing muscles or bones of the forearm and/or digits (e.g., Figures 5 and 6). *C. senex* also had distinct strips of domes in the plagiopatagium and dactylopatagium major that differed in morphology from those observed in molossids and *L. cinereus*. *C. senex* possessed regular rows of closely spaced domes lining the unique unpigmented "window" structures in the wing membrane (Figure 7).

3.3 | Association with intramembranous structures

We observed an association of sensory hair distribution with the intramembranous muscles and collagen-elastin bundles (Cheney et al., 2017). The intramembranous wing muscles are lined with sensory hair domes in all species studied. Domes were situated along the plagiopatagiales muscles in all species in our sample. Plagiopatagiales are variable in number, size, and location in the plagiopatagium among species, leading to corresponding

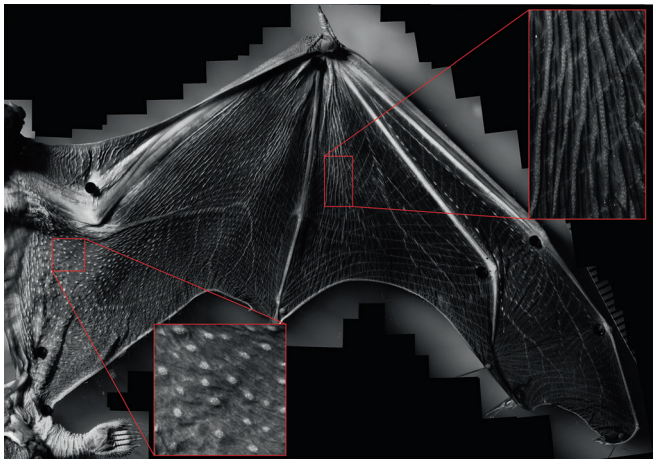

FIGURE 5 The wing of *Tadarida brasiliensis*. Sensory hairs are arranged in different configurations in different regions of the wing. Left inset: rosette-like clusters of sensory hairs. Right inset: elongated clusters, or strips, of domes.

FIGURE 6 The wing of *Lasiurus cinereus*. The close correspondence of sensory hairs with the bones of the digits is readily apparent, especially along digits III and IV (short orange arrows), and with the plagiopatagiales muscles (long blue arrow).

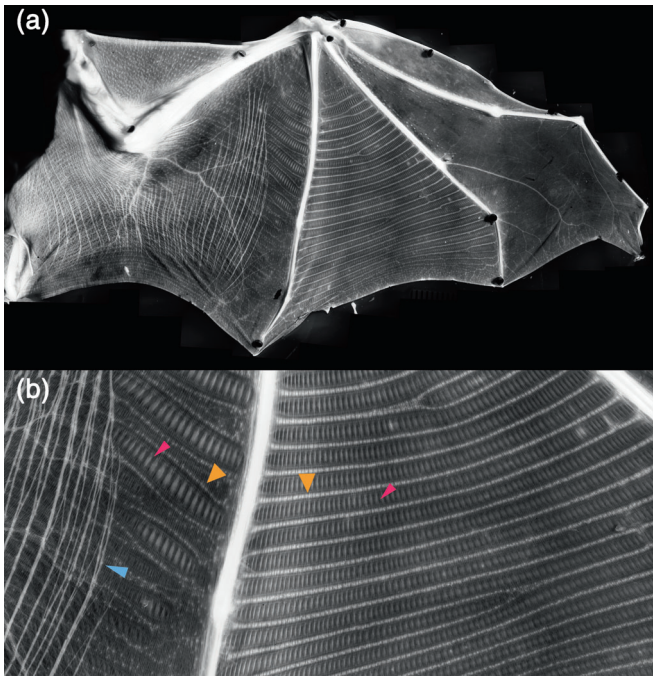

FIGURE 7 The wing of *Centurio senex (a)*. The unique translucent, window-like structures are present in the plagiopatagium distal to the plagiopatagiales muscles (blue arrow), as well as in the entire dactylopatagium major (a, b). The windows are oriented in parallel strips running span-wise along the wing (narrow pink arrows), and parallel lines of sensory hairs run between them (wide orange arrows) (b). The inset (b) shows portions of the distal plagiopatagium, dactylopatagium major, digit V, and digit IV.

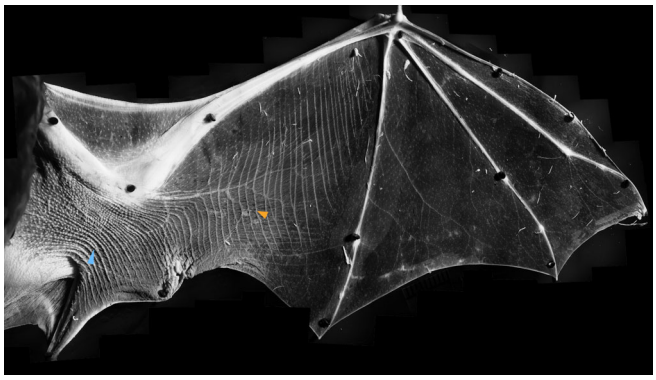

FIGURE 8 The wing of *Rhinopoma hardwickii*. Thick ridges of intramembranous wing muscles (primarily dorsopatagiales, blue arrow, and plagiopatagiales, orange arrow) are visible in the proximal plagiopatagium and are lined by sensory hairs.

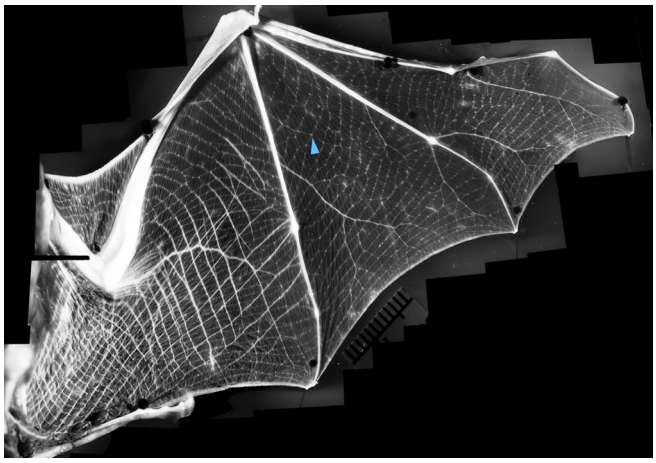

FIGURE 9 The wing of *Hipposideros bicolor*. Sensory hairs are situated at the intersections of bands of collagen and elastin (one example indicated by blue arrow).

variation in associated sensory structures (Cheney et al., 2017). Domes also lie along the dorsopatagiales muscles which run latero-caudally from the thorax and abdomen to the plagiopatagium (Figure 2) (e.g., in *L. frons*, *L. cinereus*, and *M. schmidtorum*, and others) and cubitopatagiales muscles which run a short distance laterally from origins near the elbow (Figure 2) (e.g., in *M. keaysi*, *P. davyi*, *L. frons*, and others). *R. hardwickii* has particularly robust dorsopatagiales muscles, which appear to possess large sensory hair domes; smaller domes, similar to those seen in other species, are found along its conspicuous cubitopatagiales and plagiopatagiales muscles (e.g., Figure 8).

An apparent association of the sensory hairs with collagen-elastin bundles was observed in all but the two molossid species in our sample. Domes were arranged variously along discrete tracts of connective tissue bundles in the wing (i.e., *C. brachyotis*, *C. senex*, and others); at the intersections of bundles (i.e., *H. bicolor*, *N. tumidorostris*, Figure 9); and/or ran in proximodistally-oriented bundles at the wing's leading (*M. schmidtorum*, *M. keaysi*, *N. tumidorostris*, *N. leporinus*, *P. davyi*, *S. bilineata*, *S. australis*, *and T. tricolor*) and trailing edges (*N. leporinus*, *P. davyi*, and *R. hardwickii*). In some species, the collagen-elastin bundles are arranged in a grid-like pattern, while in others their architecture is less regularly structured and more branching (see also Cheney et al., 2017). In some cases, collagen-elastin bundle patterning seemed to dictate the arrangement of domes; for example, *H. bicolor* and *N. tumidorostris* have grid-like bands of collagen-wrapped elastin in the plagiopatagium, with domes occurring only at the intersections of the bands. However, some species have domes situated between bundles of connective tissue, in "bare" wing membrane skin where there are no apparent features (i.e., *P. davyi*), as well as domes associated with the collagen-elastin bundles.

3.4 | Association with bony morphology

A subset of domes is closely associated with bones and joints of the arm- and handwing. The densities of domes immediately adjacent to joints and/or bones are elevated in at least one wing region in *C. senex*, *D. rotundus*, *L. cinereus*, *M. rufus*, *R. hardwickii*, *S. australis*, and *T. brasiliensis* (e.g., Figure 6). For example, in *S. australis*, the density of domes in the propatagium is greatest near the elbow joint. In *D. rotundus*, domes in the dactylopatagium major and minor are concentrated towards the digits, especially digit III. In *L. cinereus* domes follow digits IV and V closely, and in *M. rufus* strips of domes line digit IV. The density of domes near the digits in *D. rotundus* is higher on the distal side than the proximal side of the bones. In *C. senex*, domes are concentrated toward the digits and digital joints, especially the distal interphalangeal joint of digit IV. In *L. cinereus*, strips run parallel to digit III in the plagiopatagium; on the handwing side of the digit, in the datylopatagium major, domes and clusters run parallel to the digit. Digits III and IV are closely associated with domes in *S. australis* and strips oriented parallel to the bones in *M. rufus* and *T. brasiliensis*.

4 | DISCUSSION

Our study shows that there is substantial variation across species in the arrangement and density of the sensory hair network in bat wing membranes, which could have meaningful functional implications. In our sample, measurements of hair density ranged from fewer than 10 hairs per cm^2 in the distal regions of the wing of some species to thousands of hairs per cm^2 in some wing regions in the molossid species. Overall, our measured densities are the on same order of magnitude as densities reported in previous work for the plagio- and dactylopatagium (1–3 hairs per mm^2, Sterbing & Moss, 2018). We noted several trends in the variation in hair distribution and density among species and between wing regions. For example, sensory hair densities are higher proximally than distally, and hairs can occur singly but also in clusters or strips. Sensory hairs are often more densely concentrated near other structures in the wing, particularly the intramembranous muscles, the bones of the arm- and handwing and the collagen-elastin bundles.

4.1 | Functional implications of sensory hair organization

The density of wing sensory hairs, their overall distribution, and the specific anatomical locations of sensory hairs on the wing shapes the information communicated from the wing to the central nervous system. It is therefore reasonable to infer that the arrangement of hairs relates to their function. Previous research has proposed that the bat wing hair system serves primarily to sense airflow; that is, the hairs function as levers deflected by local airflow on the wing surface, which in turn stimulate associated sensory nerve endings in the skin (Sterbing-D'Angelo et al., 2011, 2017; Sterbing-D'Angelo & Moss, 2014). Among several types of sensory structures in bat wing membranes, diffuse endings, distinct from sensory hairs, as well as Merkel cells found near hair bases, may sense stretch (Marshall et al., 2015). We propose that sensory structures associated with hairs may additionally or alternatively function as stretch sensors, thereby serving a proprioceptive function, based on similarities with the distribution of strain-sensing structures like campaniform sensilla (CS) in the wings of most insect species (Aiello et al., 2021; Fabian et al., 2022), as well as the close association of sensory hairs and their associated domes in bat wings with intramembranous muscles.

The intramembranous wing muscles in bats originate and insert into the dermis (Cheney et al., 2017). The plagiopatagiales proprii muscles run in a craniocaudal or chordwise direction in the plagiopatagium, the membrane of the armwing, and modify camber and wing conformation during flight by altering wing stiffness, which in turn may help optimize lift and minimize drag (Cheney et al., 2014, 2022). However, the plagiopatagiales do not appear to possess the proprioceptive muscle spindles observed in virtually all mammalian skeletal muscles, with the exception of muscles of facial expression (Cobo et al., 2017; Proske & Gandevia, 2012, Swartz, unpublished data). Sensory hairs, if they function as stretch sensors that are positioned on or near intramembranous wing muscles, may transmit sensory information that would otherwise be conveyed via spindles in a typical skeletal muscle. We observed a clear association of domes with intramembranous wing muscles in all species in our study. This suggests that sensory hairs are important elements in intramembranous muscle sensorimotor pathways and may sense essential information about the state of muscle strain, which can then be relayed to the spinal cord, and up to higher levels of motor control.

Our observations also indicate a close association of sensory hairs with collagen-elastin bundles. In all but two species (molossids *M. rufus* and *T. brasiliensis*), we observed sensory hairs in proximity to collagen-elastin bundles, or situated at bundle intersections. Given its ubiquity, this association may be functionally significant. We hypothesize that sensation from connective tissue junctures may be important for the detection of strain in the wing membrane. In this conceptual framework, it may be useful to view the

sensory hair network as a sparse sensor network (Mohren et al., 2018); sensor distributions can be defined as sparse when few locations are sampled compared to the total population of locations that are not sampled. Sparse sensing theory has recently been applied with success to gain understanding of complex biological systems. Relatively complex signals can be reconstructed or classified from relatively simple patterns generated by a small subset of all possible sensors, such as whole wing strain from relatively few CS along the wing blade to sense deformation (Dickinson & Palka, 1987). Application of similar analytical approaches could reveal a potential for the bat nervous system to reconstruct load-dependent strain distributions throughout the wing from the information gained by hair sensors located along intramembranous muscles and collagen-elastin bundles.

4.2 | Sensory hairs as mechanoreceptors

The sensory hair system in bats bears superficial resemblance to the system of CS in the wings of insects in terms of their widespread distribution and arrangement along structural elements such as wing veins (Aiello et al., 2021). CS are dense in structurally significant regions, for example, near the wing hinge joint or wing base in insects, where detection of strain is helpful in overcoming inertia (Aiello et al., 2021; Ennos, 1988). Isolated CS likely convey wing strain information to the central nervous system, each firing once per wingbeat cycle at different preferred phases, to communicate wing deformations during flight (Dickinson & Palka, 1987; Mohren et al., 2018, Aiello et al., 2021). Evidence of such phase-delays in activation between individual CS suggests that these mechanosensors further provide proprioceptive information to the CNS about relative limb positioning through time (Aiello et al., 2021). Herbst corpuscles are similarly proposed as functionally important for flight control (Hörster, 1990); these specialized mechanoreceptors, which are morphologically similar to Pacinian corpuscles in mammals, are found in the wings of birds and are sensitive to rapid deformation or vibration .

We hypothesize that areas of the wing in which hair density is higher, such as the trailing edge, or areas in which sensory hairs are organized into strips or clusters, may play a relatively greater role in sensorimotor feedback than others, necessitating higher sensory bandwidth or resolution compared to wing regions with lower hair density. If noise is associated with sensory information transfer from those regions, clusters and strips may build redundancy into sensory input, or increase sensory bandwidth (Dickerson et al., 2021; Dickinson, 1990; Moran et al., 1976). Neurons that supply insect CS can fire only once per wingbeat, hence strain values from a specific sensor location provide averages over the wingbeat cycle (Fabian et al., 2022). Increasing hair density therefore may increase not only the spatial resolution of wing strain, but due to offsets in firing among neurons, may result in greater temporal resolution of the forces that influence wing deformations as well (Aiello et al., 2021). The organization of multiple sensory hairs into closely packed clusters or strips could also potentially allow the nervous system to increase the sensory resolution of average strain or flow values from a given region by increasing the density of nerve fibers throughout the wing (More et al., 2010). The presence of clusters varied among individuals and species, but several species in our sample exhibited clusters in every wing region.

4.3 | Linking sensory hair organization to flight ecology

We hypothesized that sensory hair organization would be correlated with flight ecology, but we found no significant associations of sensory hair density with feeding guild in our study. The strong relationship between wing region, species, and sensory hair density in the non-phylogenetic analysis, taken together with the mostly non-significant phylogenetic pairwise comparisons and associations with ecological proxies suggest that the data are highly structured phylogenetically. In our sample, with species drawn from across the bat phylogeny but relatively sparse sampling of specific ecologies within specific clades, phylogenetic signal may overwhelm functional or ecological signals. In addition to seeking patterns of correlation between hair distribution and density and overall ecological characterization, future work could aim to link patterning in the hair sensory network more specifically to its mechanistic function. Hypotheses that link arrangement of hairs directly to aeromechanical demands—for example, that the density of hair sensors should be higher in regions of the wing that more frequently experience detached and more turbulent airflow, or that bats whose flight repertoire incorporates a broader range of flight speeds would benefit from a greater scope of information and thus higher density in the hair network—could be tested robustly by detailed, carefully constructed interspecific comparisons. For example, of the three species that possess the most numerous and pronounced clusters and strips, *T. brasiliensis*, *M. rufus*, and *L. cinereus*, two are known to fly long distances during annual migrations. The fact that *L. cinereus*, a migratory vespertilionid, has similar sensory hair morphology to the molossids may indicate an aspect of shared functionality. All three are known for exhibiting faster, less

maneuverable flight styles than other species and for hunting mobile insect prey (McCracken et al., 2016; Shump Jr. & Shump, 1982).

There may be relationships between the distribution of wing sensory hairs and flight ecology, that is, flight behavior (foraging strategy, flight style) and morphology (wing structure) that will only become clear with larger samples and greater statistical power. Fluorescence imaging and photographic reconstruction of wing hair networks is time-intensive, resulting in a study sample of relatively few individuals of each of only 17 of over 1,400 total species of bats (Simmons & Cirranello, 2022). More robust sampling of taxa and feeding ecologies could uncover as yet hidden relationships between density, distribution, and aspects of flight ecology. Furthermore, our analysis used an approach involving ROI for averaging hair counts as a starting point, but a more intensive data collection methodology may yield further patterns. Measures of count density may also be influenced to some extent by variation in the quality of the specimens, whether or not the rigidity of fixed wings allowed for full extension of the membrane, damage to the membrane skin, and image quality. Evaluating hair density in ROI from photographs was appropriate to assess our broad hypothesis that sensory hair distribution would vary along the length of the wing and among species. Our present findings suggest that more detailed analysis will likely yield further results.

5 | CONCLUSIONS

Maneuverability and agility are hallmarks of bat flight, but difficult to quantify; the complexity of both bat flight and the distribution of sensory hairs across the wings makes it difficult to relate one to the other. This examination of the anatomical organization of the sensory hair network in a comparative context provides context for existing research on sensory hair function and highlights fruitful avenues for further research. Detailed mechanistic studies that fully map the functional performance of this component of the bat peripheral sensory system are crucial. More detailed quantification of sensory hairs across the whole surface of the wing, a comparison between dorsal and ventral hair distribution, more detailed histology and neurophysiology, and the inclusion of more functionally and phylogenetically diverse taxa would allow for a more robust analysis of sensory hair function. Understanding the functional and evolutionary significance of the complex bat wing hair sensory network will require multilevel, integrative approaches, but will provide insights that will richly repay our efforts.

AUTHOR CONTRIBUTIONS

Andrea D. Rummel: Formal analysis; investigation; methodology; supervision; visualization; writing - original draft; writing - review and editing. **Melissa M. Sierra:** Conceptualization; formal analysis; investigation; methodology; visualization; writing – original draft; writing – review and editing. **Brooke L. Quinn:** Formal analysis; visualization; writing – original draft; writing – review and editing. **Sharon M. Swartz:** Conceptualization; funding acquisition; methodology; project administration; resources; supervision; writing – review and editing.

ACKNOWLEDGMENTS

We thank Takuma Kobayashi and Emily Dai for their assistance in imaging bat wings, Dr. Beth Brainerd for the use of her laboratory for data collection, and Erika Tavares.

FUNDING INFORMATION

Supported by grants from NSF (IOS 1931135 and CMMI 1426338) to Sharon M. Swartz, the Brown University Undergraduate Teaching and Research Awards to Melissa M. Sierra, and the Bushnell Research and Education Fund to Andrea D. Rummel. Andrea D. Rummel was supported under contract FA9550-11-C-0028 and awarded by the Department of Defense, AFOSR, NDSEG Fellowship, 32 CFR 168a.

CONFLICT OF INTEREST STATEMENT

The authors declare no conflicts of interest.

DATA AVAILABILITY STATEMENT

Data will be provided in Appendix S1.

ORCID

Andrea D. Rummel https://orcid.org/0000-0003-2627-8038

Melissa M. Sierra https://orcid.org/0000-0002-0841-1619

Brooke L. Quinn https://orcid.org/0000-0002-7598-0539

Sharon M. Swartz https://orcid.org/0000-0001-5762-7435

REFERENCES

Aiello, B. R., Stanchak, K. E., Weber, A. I., Deora, T., Sponberg, S., & Brunton, B. W. (2021). Spatial distribution of campaniform sensilla mechanosensors on wings: Form, function, and phylogeny. *Current Opinion in Insect Science*, *48*, 8–17. https://doi.org/10.1016/j.cois.2021.06.002

Altshuler, D. L., Bahlman, J. W., Dakin, R., Gaede, A. H., Goller, B., Lentink, D., Segre, P. S., & Skandalis, D. A. (2015). The biophysics of bird flight: Functional relationships integrate aerodynamics, morphology, kinematics, muscles, and sensors.

Canadian Journal of Zoology, *93*, 961–975. https://doi.org/10.1139/cjz-2015-0103

Bachmann, L., Zezell, D. M., da Costa Ribeiro, A., Gomes, L., & Ito, A. S. (2006). Fluorescence spectroscopy of biological tissues—A review. *Applied Spectroscopy Reviews*, *41*, 575–590. https://doi.org/10.1080/05704920600929498

Cheney, J. A., Allen, J. J., & Swartz, S. M. (2017). Diversity in the organization of elastin bundles and intramembranous muscles in bat wings. *Journal of Anatomy*, *230*, 510–523. https://doi.org/10.1111/joa.12580

Cheney, J. A., Konow, N., Middleton, K. M., Breuer, K. S., Roberts, T. J., Giblin, E. L., & Swartz, S. M. (2014). Membrane muscle function in the compliant wings of bats. *Bioinspiration & Biomimetics*, *9*, 025007. https://doi.org/10.1088/1748-3182/9/2/025007

Cheney, J. A., Rehm, J. C., Swartz, S. M., & Breuer, K. S. (2022). Bats actively modulate membrane compliance to control camber and reduce drag. *Journal of Experimental Biology*, *225*, jeb243974. https://doi.org/10.1242/jeb.243974

Cobo, J. L., Abbate, F., de Vicente, J. C., Cobo, J., & Vega, J. A. (2017). Searching for proprioceptors in human facial muscles. *Neuroscience Letters*, *640*, 1–5. https://doi.org/10.1016/j.neulet.2017.01.016

Crowley, G. V., & Hall, L. S. (1994). Histological observations on the wing of the Grey-headed flying-Fox (Pteropus-Poliocephalus) (Chiroptera, Pteropodidae). *Australian Journal of Zoology*, *42*, 215–231. https://doi.org/10.1071/ZO9940215

Dickerson, B. H., Fox, J. L., & Sponberg, S. (2021). Functional diversity from generic encoding in insect campaniform sensilla. *Current Opinion in Physiology*, *19*, 194–203. https://doi.org/10.1016/j.cophys.2020.11.004

Dickinson, M., & Palka, J. (1987). Physiological properties, time of development, and central projection are correlated in the wing mechanoreceptors of drosophila. *The Journal of Neuroscience*, *7*, 4201–4208. https://doi.org/10.1523/JNEUROSCI.07-12-04201.1987

Dickinson, M. H. (1990). Comparison of encoding properties of campaniform sensilla on the fly wing. *Journal of Experimental Biology*, *17*, 245–261.

Dickinson, M. H., Hannaford, S., & Palka, J. (1997). The evolution of insect wings and their sensory apparatus. *Brain, Behavior and Evolution*, *50*, 13–24. https://doi.org/10.1159/000113318

Ennos, A. R. (1988). The inertial cause of wing rotation in Diptera. *Journal of Experimental Biology*, *140*, 161–169.

Fabian, J., Siwanowicz, I., Uhrhan, M., Maeda, M., Bomphrey, R. J., & Lin, H.-T. (2022). Systematic characterization of wing mechanosensors that monitor airflow and wing deformations. *iScience*, *25*, 104150. https://doi.org/10.1016/j.isci.2022.104150

Fan, X., Swartz, S., & Breuer, K. (2022). Power requirements for bat-inspired flapping flight with heavy, highly articulated and cambered wings. *Journal of the Royal Society Interface*, *19*, 20220315. https://doi.org/10.1098/rsif.2022.0315

Hörster, W. (1990). Histological and electrophysiological investigations on the vibration-sensitive receptors (Herbst corpuscles) in the wing of the pigeon (Columba livia). *Journal of Comparative Physiology A*, *166*, 663–673. https://doi.org/10.1007/BF00240016

Jones, G. (2011). Sensory biology: Bats feel the air flow. *Current Biology*, *21*, R666–R667. https://doi.org/10.1016/j.cub.2011.07.008

Marshall, K. L., Chadha, M., de Souza, L. A., Sterbing-D'Angelo, S. J., Moss, C. F., & Lumpkin, E. A. (2015). Somatosensory substrates of flight control in bats. *Cell Reports*, *11*, 851–858. https://doi.org/10.1016/j.celrep.2015.04.001

McCracken, G. F., Safi, K., Kunz, T. H., Dechmann, D. K. N., Swartz, S. M., & Wikelski, M. (2016). Airplane tracking documents the fastest flight speeds recorded for bats. *Royal Society Open Science*, *3*, 160398. https://doi.org/10.1098/rsos.160398

Mohren, T. L., Daniel, T. L., Brunton, S. L., & Brunton, B. W. (2018). Neural-inspired sensors enable sparse, efficient classification of spatiotemporal data. *Proceedings National Academy of Sciences United States of America*, *115*, 10564–10569. https://doi.org/10.1073/pnas.1808909115

Monici, M. (2005). Cell and tissue autofluorescence research and diagnostic applications. *Biotechnology Annual Review*, *11*, 227–256. https://doi.org/10.1016/S1387-2656(05)11007-2

Moran, D. T., Rowley, J. C., Zill, S. N., & Varela, F. G. (1976). The mechanism of sensory transduction in a mechanoreceptor. Functional stages in campaniform sensilla during the molting cycle. *Journal of Cell Biology*, *71*, 832–847. https://doi.org/10.1083/jcb.71.3.832

More, H. L., Hutchinson, J. R., Collins, D. F., Weber, D. J., Aung, S. K. H., & Donelan, J. M. (2010). Scaling of sensorimotor control in terrestrial mammals. *Proceedings of the Royal Society B*, *277*, 3563–3568. https://doi.org/10.1098/rspb.2010.0898

Orme, D., Freckleton, R., Thomas, G., Petzoldt, T., Fritz, S., Isaac, N., & Pearse, W. (2018). caper: Comparative analyses of Phylogenetics and evolution in R.

Owens, D. M., & Lumpkin, E. A. (2014). Diversification and specialization of touch receptors in skin. *Cold Spring Harbor Perspectives in Medicine*, *4*, a013656. https://doi.org/10.1101/cshperspect.a013656

Proske, U., & Gandevia, S. C. (2012). The proprioceptive senses: Their roles in signaling body shape, body position and movement, and muscle force. *Physiological Reviews*, *92*, 1651–1697. https://doi.org/10.1152/physrev.00048.2011

R Core Team. (2021). R: A language and environment for statistical computing.

Revell, L. J. (2012). Phytools: An R package for phylogenetic comparative biology (and other things): *Phytools: R package*. *Methods in Ecology and Evolution*, *3*, 217–223. https://doi.org/10.1111/j.2041-210X.2011.00169.x

Shi, J. J., & Rabosky, D. L. (2015). Speciation dynamics during the global radiation of extant bats. *Evolution*, *69*, 1528–1545. https://doi.org/10.1111/evo.12681

Shump, K. A., Jr., & Shump, A. U. (1982). Lasiurus cinereus. *Mammalian Species*, *185*, 1–5.

Simmons, N. B., & Cirranello, A. L. (2022). Bat species of the world: A taxonomic and geographic database. (Accessed September 11, 2022).

Sterbing, S. J., & Moss, C. F. (2018). Comparative analysis of the distribution and morphology of tactile hairs on the wing membrane of four bat species. *Journal of Mammalogy*, *99*, 124–130. https://doi.org/10.1093/jmammal/gyx146

Sterbing-D'Angelo, S., Chadha, M., Chiu, C., Falk, B., Xian, W., Barcelo, J., Zook, J. M., & Moss, C. F. (2011). Bat wing sensors support flight control. *Proceedings of the National Academy of Sciences of the United States of America*, *108*, 11291–11296. https://doi.org/10.1073/pnas.1018740108

Sterbing-D'Angelo, S. J., Chadha, M., Marshall, K. L., & Moss, C. F. (2017). Functional role of airflow-sensing hairs on the bat wing. *Journal of Neurophysiology*, *117*, 705–712. https://doi.org/10.1152/jn.00261.2016

Sterbing-D'Angelo, S. J., Liu, H., Yu, M., & Moss, C. F. (2016). Morphology and deflection properties of bat wing sensory hairs: Scanning electron microscopy, laser scanning vibrometry, and mechanics model. *Bioinspiration & Biomimetics*, *11*, 056008. https://doi.org/10.1088/1748-3190/11/5/056008

Sterbing-D'Angelo, S. J., & Moss, C. F. (2014). Air flow sensing in bats. In H. Bleckmann, J. Mogdans, & S. L. Coombs (Eds.), *Flow sensing in air and water* (pp. 197–213). Springer. https://doi.org/10.1007/978-3-642-41446-6_8

Stockwell, E. F. (2001). Morphology and flight manoeuvrability in New World leaf-nosed bats (Chiroptera: Phyllostomidae). *Journal of Zoology*, *254*, 505–514. https://doi.org/10.1017/S0952836901001005

Zook, J. M. (2005). The neuroethology of touch in bats: Cutaneous receptors of the wing. *Society for Neuroscience Abstracts*, *78*, 21.

SUPPORTING INFORMATION

Additional supporting information can be found online in the Supporting Information section at the end of this article.

How to cite this article: Rummel, A. D., Sierra, M. M., Quinn, B. L., & Swartz, S. M. (2023). Hair, there and everywhere: A comparison of bat wing sensory hair distribution. *The Anatomical Record*, 1–12. https://doi.org/10.1002/ar.25176